Tiedemann, R., Mix, A.C., Richter, C., and Ruddiman, W.F. (Eds.)
Proceedings of the Ocean Drilling Program, Scientific Results Volume 202

6. Data Report: Radiolarian Biostratigraphy, ODP Leg 202, Site 1237[1]

Mysti Weber[2] and Nicklas Pisias[2]

ABSTRACT

Site 1237 is located on Nazca Ridge ~140 km off the coast of Peru and thus within the offshore region of the Peru-Chile Current. A total of 83 samples were used to provide an initial radiolarian biostratigraphic framework for Site 1237; radiolarians are present to Sample 202-1237B-19H-2, 58–60 cm (186.45 meters composite depth [mcd]) and are of good to fair abundance and preservation. Site 1237 is influenced by both subtropical and northward-transported southern latitude waters, has 55 ash layers within the uppermost 166 m, and has minimal to gross reworking. Shipboard paleomagnetic results showed that the upper 200 m spanned the last 12 m.y., and in the upper 100 mcd, the paleomagnetic inclination pattern could be directly correlated to the geomagnetic polarity timescale (GPTS). Tropical biostratigraphy was used to establish the zonal boundaries for Site 1237, and the paleomagnetic and radiolarian stratigraphy were well correlated.

INTRODUCTION

Leg 202 of the Ocean Drilling Program (ODP) sailed without a radiolarian micropaleontologist in the scientific party. When initial shipboard analysis showed that Site 1237 may provide an excellent biostratigraphic reference for the southeast Pacific, a small-scale sampling strategy was developed to add radiolarian stratigraphy postcruise.

Site 1237 is located at 16°0.421′S, 76°22.685′W at a water depth of 3212 m. The site is on a relatively flat bench on the Nazca Ridge ~140

[1]Weber, M., and Pisias, N., 2006. Data report: radiolarian biostratigraphy, ODP Leg 202, Site 1237. *In* Tiedemann, R., Mix, A.C., Richter, C., and Ruddiman, W.F. (Eds.), *Proc. ODP, Sci. Results,* 202: College Station, TX (Ocean Drilling Program), 1–29. doi:10.2973/odp.proc.sr.202.213.2006
[2]College of Oceanic and Atmospheric Sciences, Oregon State University, 104 Ocean Administration Building, Corvallis OR 97331-5503, USA. Correspondence author: **weber@coas.oregonstate.edu**

Initial receipt: 15 July 2005
Acceptance: 22 May 2006
Web publication: 7 November 2006
Ms 202SR-213

km off the coast of Peru and near the eastern edge of the northward-flowing Peru-Chile Current (PCC), a major conduit of cool-water transport from high to low latitude, and productive upwelling system (Shipboard Scientific Party, 2003).

Ocean currents associated with Site 1237 include (1) the northward-flowing PCC, a current that transitions into the South Equatorial Current; (2) Antarctic Intermediate Water, a northward-flowing subsurface current high in oxygen and low in both salinity and nutrients (above 1 km depth); (3) Circumpolar Deep Water, an oxygen-rich northward-flowing bottom water (below 3 km); and (4) Pacific Central Water, a southward-flowing mid-depth water characterized by relatively low oxygen and salinity and high nutrients (Shipboard Scientific Party, 2003). Subtropical water from the Equatorial Undercurrent influences water upwelled along the South American coast. Thus, the oceanography of the site is influenced by both subtropical waters as well as waters transported northward from higher southern latitudes.

Shipboard paleomagnetic results showed that the upper 200 m of sediment spanned the last 12 m.y. (Shipboard Scientific Party, 2003). In the upper 100 meters composite depth (mcd), the paleomagnetic inclination pattern could be directly correlated to the geomagnetic polarity timescale (GPTS) of Cande and Kent (1995) to the base of the Gilbert Chron 3n (5.32 Ma). Ages assigned based on these correlations are in good agreement with shipboard biostratigraphy based on diatoms, coccoliths, and foraminifers. From 100 to 160 mcd, the correlation of the inclination pattern between holes and with the GPTS are less clear. However, by stacking and smoothing the multihole natural remanent magnetization (NRM) intensities, a stacked record could be correlated to the GPTS (Cande and Kent, 1995; Shipboard Scientific Party, 2003). Below 160 mcd, the increase in NRM intensity improved the sedimentary polarity change record for this interval and is easily interpreted and correlated to the GPTS. The predominant normal polarity interval between ~175 and 181 mcd is correlated to Chron C5n. Not only are the polarity chrons identifiable, but also a consistent pattern of polarity transitions is observed between Chron C4r (~162 mcd) and Chron C5Ar (~199 mcd). All polarity chrons and subchrons are identifiable within this interval, providing exceptional stratigraphic control (Shipboard Scientific Party, 2003).

METHODS

Eighty-three samples were used to provide an initial radiolarian biostratigraphic framework for Site 1237. Samples were taken along the Site 1237 composite depth scale and sampling splice as defined by the Shipboard Scientific Party (2003). On average, one sample per section from the top of the core at Sample 202-1237B-1H-1, 59–61 cm (0.59 mcd) to 7H-6, 59–61 cm (66.68 mcd) was processed and studied. One to three samples per core were processed from Sample 202-1237B-7H-6, 59–61 cm (66.68 mcd), through Sample 15H-2, 59–61 cm (143.64 mcd), at 1- to 2-m sampling intervals. In the lowermost section of the site, from Sample 202-1237B-15H-2, 59–61 cm (143.64 mcd), through 34H-1, 59–61 cm (310.09 mcd), sediments were sampled at ~10-m intervals (Table T1).

Samples were processed following the procedure described by Roelofs and Pisias (1986). The samples were treated with 50% hydrochloric acid to remove calcium carbonate, 33% hydrogen peroxide and potassium

T1. Radiolarian species range chart, p. 23.

dichromate to remove organic carbon, and finally sieved with water at 63 µm to remove the fine fraction. The 63-µm size fraction was randomly strewn on cover slips, dried, and mounted on slides with Canada balsam.

Two slides were processed for each sample and scanned at 100%. All samples above Sample 202-1237B-19H-2, 58–60 cm (186.45 mcd), contained a minimum of 500 radiolarians. Below that depth radiolarians were rare and sediments contained no stratigraphic radiolarians. Radiolarians were identified to the species level. When a radiolarian species identification was questionable, that species' characteristics were measured and confirmed by comparison to the most relevant published data. The radiolarian species presence and abundance was recorded using the system presented by Moore (1995) as follows:

R = rare (<10 specimens),
X = present (10 –100 specimens),
C = common (>100–200 specimens),
A = abundant, (>200 specimens), and
— = looked for but not found.

The one modification to this system was the change of F = few to X = present and is used to indicate that when the species was present, it was present in consistent numbers throughout the core. In addition to qualitative abundance evaluations, overall preservation was designated using numerals between 1 and 5 where

1 = very poor,
2 = poor,
3 = fair,
4 = good, and
5 = very good; and

diversity was qualitatively estimated using a scale of 1 to 5 (Table **T1**) with

1 = 29 species,
2 = 30 species,
3 = 40 species,
4 = 50 species, and
5 = 90 species.

RESULTS

In general, the abundance and preservation of radiolarians are very good at Site 1237 from the top of the core through Sample 202-1237B-6H-4, 59–61 cm (54.33 mcd). Radiolarians are present in lesser abundances and not as well preserved from Sample 202-1237B-6H-4, 59–61 cm (54.33 mcd), through 19H-2, 58–60 cm (186.45 mcd). Below 186.45 mcd, the core is barren of radiolarians; diatoms are also absent in this lower interval of the site (Shipboard Scientific Party, 2003).

As expected from the surface oceanography of the site, a combination of tropical and mid-latitude radiolarians are present at Site 1237. Site 1237 is located in the overlap of Molina-Cruz's (1977) "Peru" current and "Backwater" species assemblages. It is in an area where the upwelling process mixes cool, nutrient-rich waters into the Peru Current

and effects a unique radiolarian assemblage which is different from either the equatorial or subtropical waters (Molina-Cruz, 1977).

Mid-latitude radiolarian species found at Site 1237 include several species from the western mid-latitude Pacific Ocean (Caulet, 1986): *Lamprocyrtis daniellae* Caulet, 1986; *Phormostichoartus pitomorphus* Caulet, 1986; and *Acrosphaera spinosa fasciculopora* Caulet, 1986. Caulet described *L. daniellae* as a mid-latitude morphotype of *Lamprocyrtis nigriniae* Kling, 1977. *L. nigriniae* is also present at Site 1237; the last occurrence (LO) of *L. daniellae* is preceded by the first occurrence (FO) of *L. nigriniae*. Although Nigrini and Caulet (1988) found *Anthocyrtidium prolatum* Nigrini and Caulet, 1988, in the western tropical Pacific Ocean but not at their central Pacific Ocean site and Sanfilippo and Nigrini (1998) held that *A. prolatum* was not found in the Pacific Ocean, this species was found at Site 1237 but was not used in the biostratigraphy except to confirm relative ages. The exclusion of *A. prolatum* in studies by Johnson and Nigrini (1985) and Moore (1995) also suggests that *A. prolatum* is, if present, very rare in the eastern Pacific.

Cycladophora divisiana (Ehrenberg) Petrushevskaya, 1967; *L. nigriniae; Plectacantha cremastoplegma* Nigrini, 1968; *Dictyophimus infabricatus,* Nigrini, 1968; *Lamprocyclas maritalis ventricosa* Nigrini, 1968; *Acrosphaera murrayana* (Haeckel) group Nigrini and Caulet, 1992; and *Phormostichoartus crustula* Caulet, 1979, are radiolarian species endemic to areas of upwelling (Nigrini and Caulet, 1992). These radiolarians are represented throughout the core within each species' extant range. In general, upwelling was indicated when *C. divisiana* was very common (>35 individuals per sample) or *L. nigriniae, P. cremastoplegma, D. infabricatus, L. m. ventricosa, A. murrayana,* or *P. crustula* were present (1–20 individuals per sample).

Reworking

Some reworking was found intermittently at depths of 59.91 mcd (Sample 202-1237C-6H-6, 59–61 cm), 73.34 mcd (Sample 202-1237B-8H-4, 59–61 cm), 74.85 mcd (Sample 202-1237B-8H-5, 59–61 cm), 75.12 mcd (Sample 202-1237C-8H-3, 12–14 cm), and 78.61 mcd (Sample 202-1237D-5H-3, 12–14 cm); reworking is then continuous to 186.45 mcd (Sample 202-1237B-19H-2, 58–60 cm) (~10.945 Ma). The presence of *Didymocyrtis prismatica* (Haeckel, 1887) Sanfilippo and Riedel, 1980, found at depths of 55.83 mcd (Sample 202-1237B-6H-5, 59–61 cm) and 56.89 mcd (Sample 202-1237C-6H-4, 59–61 cm) indicated reworking from the late Oligocene/early Miocene to the late Pliocene. This is consistent with the reworking of Eocene–Oligocene diatoms into the upper Pliocene *Nitzschia marina* Zone, which was reported in Sample 202-1237B-6H-5, 70 cm (50.2 mcd) (Shipboard Scientific Party, 2003). Moore (1995) showed an inverse correlation to sedimentation rate and abundance of older radiolarians in younger sediments; the faster the accumulation of sediment, the less reworking was evident in the core. Moore (1995) also found that generally the age of the oldest reworked radiolarian present was never older than the maximum age indicated for the site.

Volcanic Ash Layers

Very high abundances of volcanic ash were found in seven of our radiolarian samples: at 30.98 mcd (Sample 202-1237D-3H-5, 59–61 cm), 54.330 mcd (Sample 202-1237B-6H-5, 59–61 cm), 58.40 mcd (Sample

202-1237C-6H-5, 59–61 cm), 68.38 mcd (Sample 7H-5, 59–61 cm), 69.88 mcd (Sample 7H-6, 59–61 cm), 98.67 mcd (Sample 10H-5, 10–12 cm), and 138.53 mcd (Sample 14H-2, 67–69 cm). These potential ash layers were not recorded in the Site 1237 preliminary data (Table T2). In addition, we found two radiolarian samples with very high abundances of volcanic ash in Samples 202-1237C-4H-4, 59–61 cm (34.86 mcd), and 7H-4, 59–61 cm (66.886 mcd), that can be correlated to ash layers found in other holes of the site. Ash layers reported in the Hole 1237B in Samples 202-1237B-4H-4, 79–86 cm (34.130 mcd), and 7H-6, 85–88 cm (66.94 mcd), correlate to the above radiolarian samples, respectively, and are likely the same ash layers found in Hole 1237B (see table T9 in Shipboard Scientific Party, 2003). The ash layers at 54.33 mcd and 58.40 mcd are above and below the area of reworking from the early Oligocene/late Miocene at 55.83 mcd (Sample 202-1237B-6H-5, 59–61 cm) and 56.89 mcd (Sample 202-1237C-6H-4, 59–61 cm), respectively, and may be associated with that sediment disturbance event.

T2. Ash layer data, p. 26.

Zonation

Two published radiolarian zonations were considered to be appropriate for Site 1237:

1. The zonation of Moore's 1995 extensive study on radiolarians in the eastern tropical Pacific, ODP Leg 138.
2. The tropical zonation of Sanfilippo and Nigrini (1998).

Moore's (1995) zonation differs only slightly from Sanfilippo and Nigrini (1998) in that Moore developed radiolarian zones that are unique to ODP Leg 138 studies and he used the older Cande and Kent (1992) geomagnetic stratigraphy, which is slightly different than the revised Cande and Kent (1995) geomagnetic stratigraphy. More importantly, paleomagnetic stratigraphy was only available on a few low-sedimentation Leg 138 sites, but the rather detailed chronology was available based on orbital tuning of sediment geochemical signals (Shackleton et al., 1995).

Primary differences in the zonal definitions of these two studies are

1. The RN11 *Lychnodictyum audax* interval zone of Sanfilippo and Nigrini (1998), which is approximately equivalent to the *Anthocyrtidium jenghisi* Zone of Moore (1995). The top this zone is defined by the LO of *Stichocorys peregrina,* and the base of the zone is defined by the LO of *Phormostichoartus doliolum*.
2. Sanfilippo and Nigrini (1998) split Zones RN12 and RN11 into interval subzones recognized only in the Indian Ocean. These subzones were not used in this study.

The two zonations are illustrated, along with the zonation defined for Site 1237, in Figure F1. The formal definitions of these zones are given below.

Sanfilippo and Nigrini (1998) developed their radiolarian biostratigraphic system for low latitudes so it is correlated to the GPTS of Cande and Kent (1995). Because of the location of Site 1237 and the presence of many tropical biostratigraphic species, it was determined that the tropical biostratigraphy was most suitable. Sanfilippo and Nigrini (1998) also suggested the development of an exclusive biostratigraphy for local and regional sites; however, Site 1237 conforms reasonably

F1. Zonations, p. 18.

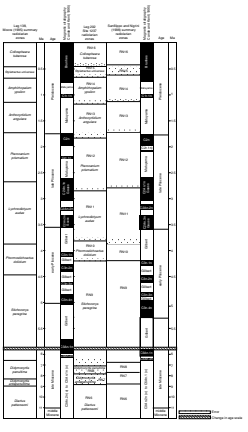

well to their zonation and thus is used as the basis for our zonation of Site 1237. Four species extinction or appearance events were used to estimate a radiolarian-based chronology for Site 1237: the LO of *Stylatractus universus* (0.42 Ma), the LO of *S. peregrina* (2.76 Ma), the evolutionary transition interval between *S. peregrina* and *Stichocorys delmontensis* (6.71 Ma), and the LO of *Diartus hughesi* (7.70 Ma) (Sanfilippo et al., 1985; ages determined from Sanfilippo and Nigrini, 1998). For these four radiolarian datums we can construct an estimated age-depth relationship for the site. In Figure **F2** the age of each sample studied is estimated using these four radiolarian datums and compared to the paleomagnetic chron ages of Site 1237 (Shipboard Scientific Party, 2003). The agreement is excellent (R^2 = 0.9923). Given that the paleomagnetic chron ages are so well correlated to the radiolarian biostratigraphic ages, it was decided that we would use the paleomagnetic chronology ages to estimate missing parts of the radiolarian zonation. Five zonal boundaries that could not be identified directly from missing first or last appearances of indicator species were estimated based on the paleomagnetic chronology.

Using the paleomagnetic data from Site 1237 we can estimate the ages of all radiolarian datums; Table **T3** compares radiolarian biostratigraphic events of Site 1237 estimated from the paleomagnetic record and published ages of radiolarian biostratigraphic events. The correlation between the published radiolarian ages and the estimated radiolarian ages at Site 1237 is very good (R^2 = 0.9823) (Fig. **F3**).

Overall ages at Site 1237 agree well with Moore (1995) (R^2 = 0.9625) and Sanfilippo and Nigrini (1998) (R^2 = 0.991) (Table **T3;** Fig. **F4**). The average of the absolute values of differences is 291 k.y. with the largest difference found for the FO of *Anthocyrtidium ehrenbergi* (difference = 1415 k.y.) and the *Diartus petterssoni* to *D. hughesi* transition (difference = 740 k.y.).

Zonal Definitions

Figure **F5** shows the zonation of Site 1237 based on our radiolarian analysis. In Figure **F5,** dashed lines denote estimated zonal boundaries, whereas solid lines indicate zones represented by the radiolarian species of Sanfilippo and Nigrini (1998). The zonation for Site 1237 is defined following Sanfilippo and Nigrini (1998) as follows.

Zone RN17 (*Buccinosphaera invaginata* Taxon-Range Zone)

Author: Nigrini (1971)
Remarks: This zone was not found at Site 1237. The core sampling began at a depth of 0.59 mcd; it is possible that Zone RN17 was not sampled.

Zone RN16 (*Collosphaera tuberosa* Interval Zone)

Author: Nigrini (1971)
Top: FO of *Buccinosphaera invaginata*
Base: LO of *Stylatractus universus*
Interval: Sample 202-1237D-1H-6, 59–61 cm (10.42 mcd), through Sample 202-1237C-2H-3, 59–61 cm (11.80 mcd).
Remarks: *B. invaginata* was not found at Site 1237 (see "Zone RN17," p. 6, remarks).

F2. Paleomagnetic and calculated radiolarian ages, p. 19.

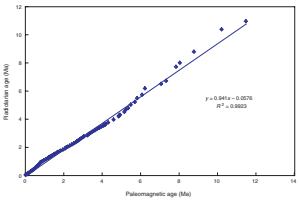

T3. Median species ages, p. 29.

F3. Published and Site 1237 radiolarian datums, p. 20.

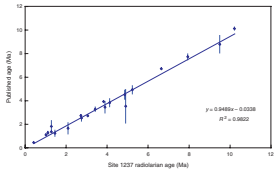

F4. Moore, Sanfilippo and Nigrini, and Site 1237 radiolarian datums, p. 21.

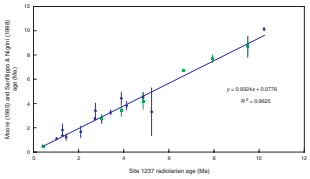

F5. Radiolarian biostratigraphy range chart, p. 22.

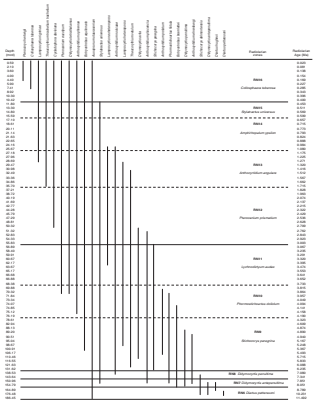

Zone RN15 (*Stylatractus universus* Interval Zone Concurrent Range Zone)

Author: Caulet (1979); renamed by Johnson et al. (1989)
Top: LO of *Stylatractus universus*
Top interval: Sample 202-1237D-1H-6, 59–61 cm (10.42 mcd), through Sample 202-1237C-2H-3, 59–61 cm (11.80 mcd).
Base: FO of *Collosphaera tuberosa*
Base interval: Sample 202-1237D-2H-2, 59–61 cm (15.59 mcd), through Sample 202-1237D-2H-3, 59–61 cm (17.10 mcd).
Remarks: *C. tuberosa* was found only in Sample 202-1237D-1H-4, 59–61 cm (7.41 mcd). The base age of this zone was estimated using paleomagnetic chronology ages of Site 1237 (Shipboard Scientific Party, 2003).

Zone RN14 (*Amphirhopalum ypsilon* Interval Zone)

Author: Nigrini (1971)
Top: FO of *Collosphaera tuberosa*
Top interval: Sample 202-1237D-2H-2, 59–61 cm (15.59 mcd), through Sample 2H-3, 59–61 cm (17.10 mcd).
Base: LO of *Anthocyrtidium angulare*
Base interval: Sample 202-1237C-3H-4, 59–61 cm (25.67 mcd), through Sample 3H-5, 59–61 cm (27.18 mcd).
Remarks: *C. tuberosa* was found only in Sample 202-1237D-1H-4, 59–61 cm (7.41 mcd). *A. angulare,* the species defining the bottom of interval Zone RN14, is not present. The top and base of this zone were estimated using paleomagnetic chronology ages of Site 1237 (Shipboard Scientific Party, 2003). The base of this zone is confirmed by the LO of *Lamprocyrtis neoheteroporos* (Kling, 1973) (Anderson, et al., 1988) and *Anthocyrtidium nosicaae* (Caulet, 1979) (Nigrini and Caulet, 1988). *A. nosicaae* is a species with an LO of ~1.00 Ma and is approximately concurrent with the LO of *A. angulare* (Nigrini and Caulet, 1988).

Zone RN13 (*Anthocyrtidium angulare* Interval Zone)

Author: Nigrini (1971)
Top: LO of *Anthocyrtidium angulare*.
Top interval: Sample 202-1237C-3H-4, 59–61 cm (25.67mcd), through Sample 3H-5, 59–61 cm (27.18 mcd).
Base: LO of *Pterocanium prismatium*.
Base interval: Sample 202-1237D-4H-2, 59–61 cm (35.70 mcd), through Sample 4H-3, 59–61 cm (37.21 mcd).
Remarks: *A. angulare* and *P. prismatium* were not found at Site 1237. The top and base of this zone were estimated using paleomagnetic chronology ages of Site 1237. The FO of *Lamprocyrtis nigriniae* and the LO of *Lamprocyrtis heteroporos* occur in this zone and are consistent with the zonation of Sanfilippo and Nigrini (1998). The transition of *Theocorythium trachelium trachelium* to *Theocorythium vetulum* occurs in the lowermost portion of this zone at Site 1237 and is a slightly younger event than the transition from *T. t. trachelium* to *T. vetulum* in Zone RN12 of Sanfilippo and Nigrini (1998) (Table T3).

Zone RN12 (*Pterocanium prismatium* Interval Zone)

Author: Riedel and Sanfilippo (1970); emend. Riedel and Sanfilippo (1978); emend. Sanfilippo et al. (1985)
Top: LO of *Pterocanium prismatium*.
Top interval: Sample 202-1237D-4H-2, 59–61 cm (35.70 mcd), through Sample 4H-3, 59–61 cm (37.21 mcd).
Base: LO of *Stichocorys peregrina*.
Base interval: Sample 202-1237C-6H-4, 59–61 cm (56.89 mcd), through Sample 6H-5, 59–61 cm (58.40 mcd).
Remarks: *P. prismatium* is not present at Site 1237. The top of this zone was estimated using paleomagnetic chronology ages of Site 1237 (Shipboard Scientific Party, 2003). The FO of *C. divisiana* occurs in this zone and is consistent with the zonation of Sanfilippo and Nigrini (1998).

Zone RN11 (*Lychnodictyum audax* Interval Zone)

Author: Sanfilippo and Nigrini (1998)
Top: LO of *Stichocorys peregrina*.
Top interval: Sample 202-1237C-6H-4, 59–61 cm (56.89 mcd), through Sample 6H-5, 59–61 cm (58.40 mcd).
Base: LO of *Phormostichoartus doliolum*.
Base interval: Sample 202-1237C-7H-5, 59–61 cm (68.38 mcd), through Sample 7H-6, 59–61 cm (69.88 mcd).
Remarks: *P. doliolum* was not found at Site 1237; the bottom of the zone boundary was estimated using paleomagnetic chronology ages of Site 1237 (Shipboard Scientific Party, 2003).

Zone RN10 (*Phormostichoartus doliolum* Interval Zone)

Author: Johnson et al. (1989); emend. Moore (1995)
Top: LO of *Phormostichoartus doliolum*.
Top interval: Sample 202-1237C-7H-5, 59–61 cm (68.38 mcd), through Sample 7H-6, 59–61 cm (69.88 mcd).
Base: LO of *Didymocyrtis penultima*.
Base interval: Sample 202-1237D-5H-1, 72–74 cm (76.19 mcd), through Sample 5H-3, 12–14 cm (78.610 mcd).
Remarks: *P. doliolum* was not found at Site 1237; the top of the zone boundary was estimated using paleomagnetic chronology ages of Site 1237 (Shipboard Scientific Party, 2003).

Zone RN9 (*Stichocorys peregrina* Interval Zone)

Author: Riedel and Sanfilippo (1970); emend. Riedel and Sanfilippo (1978)
Top: LO of *Didymocyrtis penultima*.
Top interval: Sample 202-1237D-5H-1, 72–74 cm (76.19 mcd), through Sample 5H-3, 12–14 cm (78.610 mcd).
Base: Evolutionary transition from *S. delmontensis* to *S. peregrina*.
Base interval: Sample 202-1237C-13H-5, 58–60 cm (131.62 mcd), through Sample 14H-2, 67–69 cm (138.53 mcd).

Zone RN8 (*Didymocyrtis penultima* Interval Zone)

Author: Riedel and Sanfilippo (1970); emend. Riedel and Sanfilippo (1978)
Top: Evolutionary transition from *S. delmontensis* to *S. peregrina*.
Top interval: Sample 202-1237C-13H-5, 58–60 cm (131.62 mcd), through Sample 14H-2, 67–69 cm (138.53 mcd).
Base: LO of *Diartus hughesi*.
Base interval: Sample 202-1237C-15H-4, 58–60 cm (143.64 mcd), through Sample 15H-4, 58–60 cm (150.96 mcd).

Zone RN7 (*Didymocyrtis antepenultima* Interval Zone)

Author: Riedel and Sanfilippo (1970); emend. Riedel and Sanfilippo (1978)
Top: LO of *Diartus petterssoni*.
Top interval: Sample 202-1237C-15H-4, 58–60 cm (143.64 mcd), through Sample 15H-4, 58–60 cm (150.96 mcd).
Base: Evolutionary transition from *D. petterssoni* to *D. hughesi;* diachronous event (Johnson and Nigrini, 1985).
Base interval: Sample 202-1237B-16H-3, 58–60 cm (154.79 mcd), through Sample 17H-2, 58–60 cm (164.89 mcd).

Zone RN6 (*Diartus petterssoni* Interval Zone)

Author: Riedel and Sanfilippo (1970); emend. Riedel and Sanfilippo (1978)
Top: Evolutionary transition from *D. petterssoni* to *D. hughesi;* diachronous event (Johnson and Nigrini, 1985).
Top interval: Sample 202-1237B-16H-3, 58–60 cm (154.79 mcd), through Sample 17H-2, 58–60 cm (164.89 mcd).
Base: FO of *D. petterssoni;* diachronous event (Johnson and Nigrini, 1985).
Base interval and last sample containing radiolarians: Sample 202-1237B-19H-2, 58–60 cm (186.45 mcd).

SUMMARY

Site 1237 is in an area of upwelling and is influenced by both subtropical water as well as water transported northward from higher southern latitudes.

The shipboard paleomagnetic results based on the GPTS of Cande and Kent (1995) are in good agreement with the biostratigraphy of radiolarians studied at Site 1237 and with the biostratigraphic zonation set forth by Sanfilippo and Nigrini (1998) and Moore (1995). Although several marker species were not present, paleomagnetic age estimates are used to define the age boundaries of the radiolarian zonation and are used to estimate the age of 21 radiolarian datums in the southeastern Pacific Ocean. Reworking was generally minor and did not affect the radiolarian biostratigraphy at the site. Reworking from the Eocene–Miocene was found in one radiolarian sample and also found at about the same depth and age as in the shipboard diatom studies. Shipboard studies tabulated 55 ash layers at the site; many of these ash layers could be correlated to the radiolarian samples studied. Abundant ash was found

in several radiolarian samples in holes that were not noted in the shipboard preliminary studies but could be found in corresponding holes at the site.

ACKNOWLEDGMENTS

We wish to thank the Integrated Ocean Drilling Program and the Leg 202 Scientific Party. This research used samples and/or data provided by the Ocean Drilling Program (ODP). ODP is sponsored by the U.S. National Science Foundation (NSF) and participating countries under management of Joint Oceanographic Institutions (JOI). Funding for this research was provided by OCE9530094.

REFERENCES

Anderson, O.R., Hays, J.D., and Gross, M., 1988. An ontogenetic analysis of changes in morphology during phylogeny of some *Lamprocyrtis* spp. from deep sea sediments. *Micropaleontology,* 34(1):41–51. **doi:10.2307/1485609**

Bailey, J.W., 1856. Notice of microscopic forms found in the soundings of the Sea of Kamtschatka—with a plate. *Am. J. Sci.,* 22:1–6.

Campbell, A.S., and Clark, B.L., 1944. Miocene radiolarian faunas from southern California. *Spec. Pap.—Geol. Soc. Am.,* 51:1–76.

Cande, S.C., and Kent, D.V., 1992. A new geomagnetic polarity time scale for the Late Cretaceous and Cenozoic. *J. Geophys. Res.,* 97(10):13917–13951.

Cande, S.C., and Kent, D.V., 1995. Revised calibration of the geomagnetic polarity timescale for the Late Cretaceous and Cenozoic. *J. Geophys. Res.,* 100(B4):6093–6095. **doi:10.1029/94JB03098**

Caulet, J.-P., 1971. Contribution a l'étude de quelques radiolaries nassellaires des boues de la Méditerranée et du Pacifique (Study of some nassellarian radiolaria from Mediterranean and Pacific sediments). Archives originale, Centre de Documentation, C.N.R.S., No. 498. *Cah. Micropaleontol.,* Ser. 2, 10:1–10.

Caulet, J.-P., 1979. Les depots a Radiolaires d'age Pliocene superieur a Pleistocene dans l'ocean Indien central: nouvelle zonation biostratigraphique (Radiolarian upper Pliocene–Pleistocene deposits in the central Indian Ocean; new biostratigraphic zonation). *Mem. Mus. Nat. Hist., Nat. Ser. C (Paris),* 43:119–141.

Caulet, J.P., 1986. Radiolarians from the southwest Pacific. *In* Kennett, J.P., von der Borch, C.C., et al., *Init. Repts. DSDP,* 90: Washington (U.S. Govt. Printing Office), 835–861.

Ehrenberg, C.G., 1861. Elemente des tiefen Meeresgrundes in Mexikanischen Golfstrome bei Florida; Ueber die Tiefgrund-Verhältnisse des Oceans am Eingang der Davisstrasse und bei Island. *K. Preuss. Akad. Wiss. Ber-lin, Monatsber.,* 222–240, 275–315.

Ehrenberg, C.G., 1872a. Mikrogeologische Studien als Zusammenfassung der Beobachtungen des kleinsten Lebens der Meeres-Tiefgrunde aller Zonen und dessen geologischen Einfluss. *K. Preuss. Akad. Wiss. Berlin, Monatsberichte,* 1872:265–322.

Ehrenberg, C.G., 1872b. Mikrogeologische Studien über das kleinste Leben der Meeres-Tiefgrunde aller Zonen und dessen geologischen Einfluss. *Abh. K. Akad. Wiss. Berlin,* 1872:131–399.

Haeckel, E., 1887. Report on the radiolaria collected by H.M.S. *Challenger* during the years 1873–1876. *Rep. Sci. Results Voy. H.M.S.* Challenger, *1873–1876, Zool.,* 18:1–1803.

Hays, J.D., 1965. Radiolaria and late Tertiary and Quaternary history of Antarctic seas. *In* Llano, G.A. (Ed.), *Biology of the Antarctic Seas II.* Antarct. Res. Ser., 5:125–184.

Hays, J.D., 1970. Stratigraphy and evolutionary trends of radiolaria in North Pacific deep sea sediments. *In* Hays, J.D. (Ed.), *Geological Investigations of the North Pacific.* Mem.—Geol. Soc. Am., 126:185–218.

Johnson, D.A., and Nigrini, C.A., 1985. Synchronous and time-transgressive Neogene radiolarian datum levels in the equatorial Indian and Pacific Oceans. *Mar. Micropaleontol.,* 9(6):489–524. **doi:10.1016/0377-8398(85)90015-5**

Johnson, D.A., Schneider, D.A., Nigrini, C.A., Caulet, J.-P., and Kent, D.V., 1989. Pliocene–Pleistocene radiolarian events and magnetostratigraphic calibrations for the tropical Indian Ocean. *Mar. Micropaleontol.,* 14(1–3):33–66. **doi:10.1016/0377-8398(89)90031-5**

Kling, S.A., 1973. Radiolaria from the eastern North Pacific, Deep Sea Drilling Project, Leg 18. *In* Kulm, L.D., von Huene, R., et al., *Init. Repts. DSDP,* 18: Washington (U.S. Govt. Printing Office), 617–671.

Kling, S.A., 1977. Local and regional imprints on radiolarian assemblages from California coastal basin sediments. *Mar. Micropaleontol.,* 2:207–221. **doi:10.1016/0377-8398(77)90011-1**

Knoll, A., and Johnson, D.A., 1975. Late Pleistocene evolution of the collosphaerid radiolarian *Buccinosphaera invaginata* Haeckel. *Micropaleontology,* 21(1):60–68. **doi:10.2307/1485155**

Molina-Cruz, A., 1977. Radiolarian assemblages and their relationship to the oceanography of the subtropical southeastern Pacific. *Mar. Micropaleontol.,* 2:315–352. **doi:10.1016/0377-8398(77)90016-0**

Moore, T.C., Jr., 1995. Radiolarian stratigraphy, Leg 138. *In* Pisias, N.G., Mayer, L.A., Janecek, T.R., Palmer-Julson, A., and van Andel, T.H. (Eds.), *Proc. ODP, Sci. Results,* 138: College Station, TX (Ocean Drilling Program), 191–232.

Nakaseko, K., 1963. Neogene Cyrtoidea (radiolaria) from the Isozaki Formation in Ibaraki prefecture, Japan. *Sci. Rep., Coll. Gen. Educ., Osaka Univ.,* 12:165–198.

Nigrini, C., 1967. Radiolaria in pelagic sediments from the Indian and Atlantic Oceans. *Bull. Scripps Inst. Oceanogr.,* 11:1–125.

Nigrini, C., 1968. Radiolaria from eastern tropical Pacific sediments. *Micropaleontology,* 14(1):51–63. **doi:10.2307/1484765**

Nigrini, C., 1971. Radiolarian zones in the Quaternary of the equatorial Pacific Ocean. *In* Funnell, B.M., and Riedel, W.R. (Eds.), *The Micropalaeontology of Oceans:* Cambridge (Cambridge Univ. Press), 443–461.

Nigrini, C., 1977. Tropical Cenozoic Artostrobiidae (Radiolaria). *Micropaleontology,* 23(3):241–269. **doi:10.2307/1485215**

Nigrini, C., and Caulet, J.-P., 1988. The genus *Anthocyrtidium* (radiolaria) from the tropical late Neogene of the Indian and Pacific Oceans. *Micropaleontology,* 34(4):341–360. **doi:10.2307/1485602**

Nigrini, C., and Caulet, J.P., 1992. Late Neogene radiolarian assemblages characteristic of Indo-Pacific areas of upwelling. *Micropaleontology,* 38(2):139–164. **doi:10.2307/1485992**

Nigrini, C., and Moore, T.C., 1979. *A Guide to Modern Radiolaria.* Spec. Publ.—Cushman Found. Foraminiferal Res., 16.

Petrushevskaya, M.G., 1967. Radiolyarii otryadov Spumellaria i Nassellaria antarkticheskoi oblasti (Antarctic spumellariane and nassellariane radiolarians). *In* Andriyashev, A.P., and Ushakov, P.V. (Eds.), *Rez. Biol. Issled. Sov. Antarkt. Eksped. 1955–58,* 3:5–187.

Roelofs, A.K., and Pisias, N.G., 1986. Revised technique for preparing quantitative radiolarian slides from deep-sea sediments. *Micropaleontology,* 32(2):182–185. **doi:10.2307/1485631**

Riedel, W.R., 1953. Mesozoic and late Tertiary Radiolaria of Rotti. *J. Paleontol.,* 27(6):805–813.

Riedel, W.R., 1957. Radiolaria: a preliminary stratigraphy. *In* Petterson, H. (Ed.), *Rep. Swed. Deep-Sea Exped., 1947–1948,* 6(3):59–96.

Riedel, W.R., and Sanfilippo, A., 1970. Radiolaria, Leg 4, Deep Sea Drilling Project. *In* Bader, R.G., Gerard, R.D., et al., *Init. Repts. DSDP,* 4: Washington (U.S. Govt. Printing Office), 503–575.

Riedel, W.R., and Sanfilippo, A., 1971. Cenozoic Radiolaria from the western tropical Pacific, Leg 7. *In* Winterer, E.L., Riedel, W.R., et al., *Init. Repts. DSDP,* 7 (Pt. 2): Washington (U.S. Govt. Printing Office), 1529–1672.

Riedel, W.R., Sanfilippo, A., and Cita, M.B., 1974. Radiolarians from the stratotype Zanclean (lower Pliocene, Sicily). *Riv. Ital. Paleontol. Stratigr.,* 80:699–734.

Sanfilippo, A., and Nigrini, C., 1998. Code numbers for Cenozoic low latitude radiolarian biostratigraphic zones and GPTS conversion tables. *Mar. Micropaleontol.,* 33(1–2):109–117. **doi:10.1016/S0377-8398(97)00030-3**

Sanfilippo, A., and Riedel, W.R., 1970. Post-Eocene "closed" theoperid radiolarians. *Micropaleontology,* 16(4):446–462. **doi:10.2307/1485072**

Sanfilippo, A., and Riedel, W.R., 1980. A revised generic and suprageneric classification of the Artiscins (radiolaria). *J. Paleontol.,* 54(5):1008–1011.

Sanfilippo, A., Westberg-Smith, M.J., and Riedel, W.R., 1985. Cenozoic radiolaria. *In* Bolli, H.M., Saunders, J.B., and Perch-Nielsen, K. (Eds.), *Plankton Stratigraphy:* Cambridge (Cambridge Univ. Press), 631–712.

Shackleton, N.J., Crowhurst, S., Hagelberg, T., Pisias, N.G., and Schneider, D.A., 1995. A new late Neogene time scale: application to Leg 138 sites. *In* Pisias, N.G., Mayer, L.A., Janecek, T.R., Palmer-Julson, A., and van Andel, T.H. (Eds.), *Proc. ODP, Sci. Results,* 138: College Station, TX (Ocean Drilling Program), 73–101.

Shipboard Scientific Party, 2003. Site 1237. *In* Mix, A.C., Tiedemann, R., Blum, P., et al., *Proc. ODP, Init. Repts.,* 202: College Station, TX (Ocean Drilling Program), 1–107. **doi:10.2973/odp.proc.ir.202.108.2003**

Stöhr, E., 1880. Die Radiolarienfauna der Tripoli von Grotte, Provinz Girgenti in Sicilien (The radiolarian fauna of the Tripoli of Grotte, Girgenti Province, Sicily). *Paleontographica,* 26:69–124.

APPENDIX

Species List

***Acrosphaera murrayana* (Haeckel) group Nigrini and Caulet**

Acrosphaera murrayana (Haeckel) group Nigrini and Caulet, 1992, p. 144, pl. 1, figs. 2–4.

***Acrosphaera spinosa fasciculopora* Caulet**

Acrosphaera spinosa fasciculopora Caulet. Caulet, 1986, p. 849, pl. 1, fig. 1.

***Amphirhopalum ypsilon* (Haeckel)**

Amphirhopalum ypsilon Haeckel, 1887, p. 522; Nigrini, 1967, p. 35, pl. 3, figs. 3a–3d.

***Anthocyrtidium ehrenbergi* (Stöhr) group**

Anthocyrtis ehrenbergi Stöhr. Stöhr, 1880, p. 100, pl. 3, fig., 21a, 21b.
Anthocyrtidium ehrenbergi (Stöhr). Riedel et al., 1974, p. 712, pl. 60, fig. 10; pl. 61, fig. 1.

***Anthocyrtidium nosicaae* Caulet**

Anthocyrtidium nosicaae Caulet. Caulet, 1979, p. 132, pl. 2, figs. 8, 9.

***Anthocyrtidium ophirense* (Ehrenberg)**

Anthocyrtis ophirensis Ehrenberg, 1872a, p. 301; Haeckel, 1887, p. 1270.
Anthocyrtidium ophirense Nigrini, 1967, p. 56, pl. 6, fig. 3.

***Anthocyrtidium pliocencia* (Seguenza)**

Anthocyrtis ehrenbergi Stöhr var. *pliocenica* Seguenza, in Stöhr, 1880, p. 232.
Anthocyrtidium pliocencia Nigrini and Caulet, 1988, p. 355, pl. 2, figs. 5, 6.

***Anthocyrtidium prolatum* Nigrini and Caulet**

Anthocyrtidium prolatum Nigrini and Caulet. Nigrini and Caulet, 1988, p. 355, pl. 2, figs. 7–10.

***Axoprunum stauraxonium* Haeckel**

Axoprunum stauraxonium Haeckel. Haeckel, 1887, p. 298, pl. 48, fig. 4; Hays, 1965, p. 170, pl. 1, fig. 3.

***Botryostrobus aquilonaris* (Bailey) group**

Eucyrtidium aquilonaris Bailey, 1856, p. 4, pl. 1, fig. 9.
Botryostrobus aquilonaris (Bailey) Nigrini, 1977, p. 246, pl. 1, fig. 1.

***Botryostrobus bramlettei bramlettei* (Campbell and Clark)**

Lithomitra bramlettei Campbell and Clark, 1944, p. 53, pl. 7, figs. 10–14.
Botryostrobus bramlettei bramlettei (Campbell and Clark) Caulet, 1979, p. 129, pl. 1, fig. 5.

***Buccinospheara invaginata* Haeckel**

Buccinospheara invaginata Haeckel. Haeckel, 1887, p. 99, pl. 5, fig. 11; Knoll and Johnson, 1975, p. 249, pl. 1, fig. 9.

***Collosphaera tuberosa* Haeckel**

Collosphaera tuberosa Haeckel. Haeckel, 1887, p. 97; Nigrini, 1971, p. 445, pl. 34.1, fig. 1.

***Cyrtocapsella japonica* Nakaseko**

Cyrtocapsella japonica Nakaseko. Nakaseko, 1963, p. 193, text-figs. 20–21, pl. 4, figs. 1–3.

***Cycladophora davisiana* (Ehrenberg)**

Cycladophora? *davisiana* Ehrenberg, 1861, p. 297; 1872b, pl. 2, fig. 11.
Cycladophora davisiana (Ehrenberg) Petrushevskaya, 1967, p. 122, fig. 69 (I–VII).

***Diartus hughesi* (Campbell and Clark)**

Ommatocampe hughesi Campbell and Clark, 1944, p. 23, pl. 3, fig. 12.
Diartus hughesi (Campbell and Clark) Sanfilippo and Riedel, 1980, p. 1010.

***Diartus petterssoni* (Riedel and Sanfilippo)**

Cannartus(?) *petterssoni* Riedel and Sanfilippo, 1970, p. 520, pl. 14, fig. 3.
Diartus petterssoni (Riedel and Sanfilippo) Sanfilippo and Riedel, 1980, p. 1010, text-fig.1, h.

***Dictyophimus infabricatus* Nigrini**

Dictyophimus infabricatus Nigrini. Nigrini 1968, p. 56, pl. 1, fig. 6.

***Didymocyrtis antepenultima* (Riedel and Sanfilippo)**

Ommatartus antepenultima Riedel and Sanfilippo, 1970, p. 521, pl. 14, fig. 4.
Didymocyrtis antepenultima (Riedel and Sanfilippo) Sanfilippo and Riedel, 1980, p. 1010.

***Didymocyrtis avita* (Riedel)**

Panartus avita Riedel, 1953, p. 808, pl. 84, fig. 7.
Didymocyrtis avita (Riedel) Sanfilippo and Riedel, 1980, p. 1010.

***Didymocyrtis penultima* (Riedel)**

Panarium penultimum Riedel, 1957, p. 76, pl. 1, fig. 1.
Didymocyrtis penultima (Riedel) Sanfilippo and Riedel, 1980, p. 1010, text-fig. 1, f.

***Didymocyrtis prismatica* (Haeckel)**

Pipettella prismatica Haeckel, 1887, p. 305, pl. 39, fig. 6.
Didymocyrtis prismatica (Haeckel) Sanfilippo and Riedel, 1980, p. 1010.

***Didymocyrtis tetrathalamus* (Haeckel)**

Panartus tetrathalamus Haeckel, 1887, p. 378, pl. 40, fig. 3.
Didymocyrtis tetrathalamus (Haeckel) Sanfilippo and Riedel, 1980, p. 1010, text-fig. 1, g.

***Lamprocyclas maritalis* Haeckel *ventricosa* Nigrini**

Lamprocyclas maritalis Haeckel *ventricosa* Nigrini, 1968, p. 57, pl. 1, fig. 9.

***Lamprocyrtis heteroporos* (Hays)**

Lamprocyclas heteroporos Hays, 1965, p. 179, pl. 3, fig. 1.
Lamprocyrtis heteroporos (Hays) Kling, 1973, p. 639, pl. 5, figs. 19–21; pl. 15, fig. 6.

***Lamprocyrtis neoheteroporos* Kling**

Lamprocyrtis neoheteroporos Kling, 1973, p. 639, pl. 5, fig. 17; pl. 15, figs. 4, 5.

***Lamprocyrtis nigriniae* (Caulet)**

Conarachnium nigriniae Caulet, 1971, p. 3, figs. 1–4; pl. 4, figs. 1–4.
Lamprocyrtis nigriniae (Caulet) Kling, 1977, p. 217, pl. 1, fig. 17.

***Phormostichoartus crustula* (Caulet)**

Lithamphora crustula Caulet 1979, p. 131, pl. 2, fig. 1.
Phormostichoartus crustula (Caulet) Nigrini and Caulet, 1992, p. 161, pl. 6, figs. 10–14.

***Phormostichoartus doliolum* (Riedel and Sanfilippo)**

Artostrobium doliolum Riedel and Sanfilippo, 1971, p. 1599, pl. 1H, figs. 1–3; pl. 8, figs. 14, 15.
Phormostichoartus doliolum (Riedel and Sanfilippo) Nigrini, 1977, p. 252, pl. 1, fig. 14.

***Phormostichoartus fistula* Nigrini**

Phormostichoartus fistula Nigrini. Nigrini, 1977, p. 253, pl. 1, figs. 11–13.

***Plectacantha cremastoplegma* Nigrini**

Plectacantha cremastoplegma Nigrini. Nigrini, 1968, p. 55, pl. 1, fig. 3a–3c, text-fig. 2.

***Pterocanium auritum* Nigrini and Caulet**

Pterocanium auritum Nigrini and Caulet. Nigrini and Caulet, 1992, p. 152, pl. 4, figs. 6–8.

***Pterocanium praetextum* (Ehrenberg) *eucolpum* Haeckel**

Pterocanium eucolpum Haeckel, 1887, p. 1322, pl. 73, fig. 4; Nigrini, 1967, p. 70, pl. 7, fig. 2.

***Pterocorys hertwigii* (Haeckel)**

Pterocorys hertwigii (Haeckel). Haeckel, 1887, p. 1491, pl. 80, fig. 12; Nigrini and Moore, 1979, p. N85, pl. 25, fig. 9.

***Stichocorys delmontensis* (Campbell and Clark)**

Eucyrtidium delmontense Campbell and Clark, 1944, p. 56, pl. 7, figs. 19, 20.
Stichocorys delmontensis (Campbell and Clark) Sanfilippo and Riedel, 1970, p. 451, pl. 1, fig. 9.

***Stichocorys peregrina* (Riedel)**

Eucyrtidium elongatum peregrinum Riedel, 1953, p. 812, pl. 85, fig. 2.
Stichocorys peregrina (Riedel) Sanfilippo and Riedel, 1970, p. 451, pl. 1, fig. 10.

***Stylatractus universus* Hays**

Stylatractus universus Hays, 1970, p. 215, pl. 1, figs. 1, 2.

***Theocorythium trachelium trachelium* (Ehrenberg)**

Eucyrtidium Trachelius Ehrenberg, 1872a, p. 312.
Theocorythium trachelium trachelium (Ehrenberg), Nigrini, 1967, p. 79, pl. 8, fig. 2; pl. 9, fig. 2.

***Theocorythium trachelium* (Ehrenberg) *dianae* Haeckel**

Theocorys dianae Haeckel, 1887, p. 1416, pl. 69, fig. 11.
Theocorythium trachelium (Ehrenberg) *dianae* (Haeckel), Nigrini, 1967, p. 77, pl. 8, fig. 1a, 1b; pl. 9, fig. 1a, 1b.

***Theocorythium vetulum* Nigrini**

Theocorythium vetulum Nigrini, 1971, p. 447, pl. 34.1, fig. 6a, 6b.

Figure F1. Zonations of Moore (1995), Sanfilippo and Nigrini (1998), and Shipboard Scientific Party (2003). Species interval zones were included with the zonal code numbers for clarity.

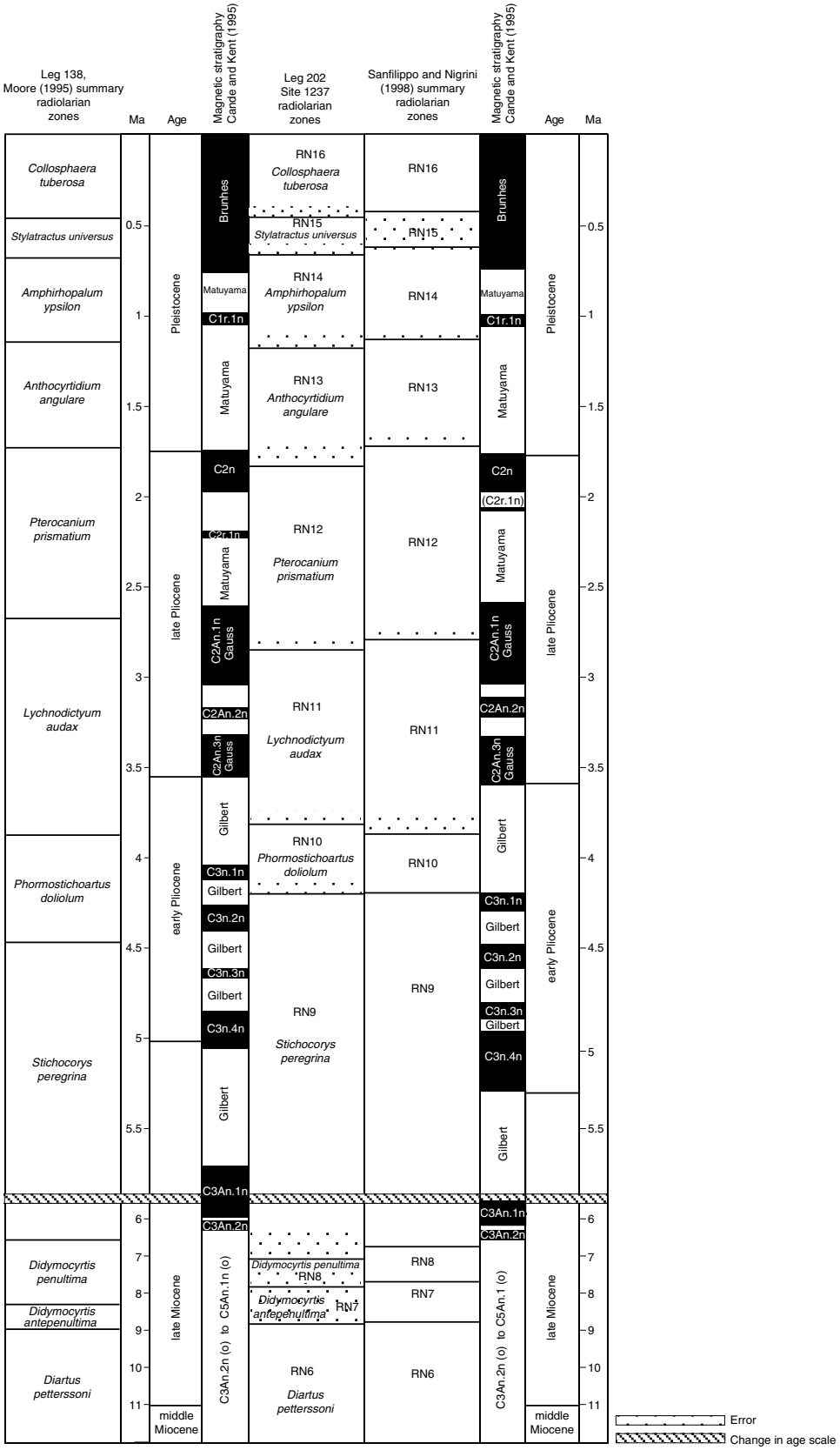

Figure F2. Leg 202, Site 1237 paleomagnetic and calculated radiolarian ages.

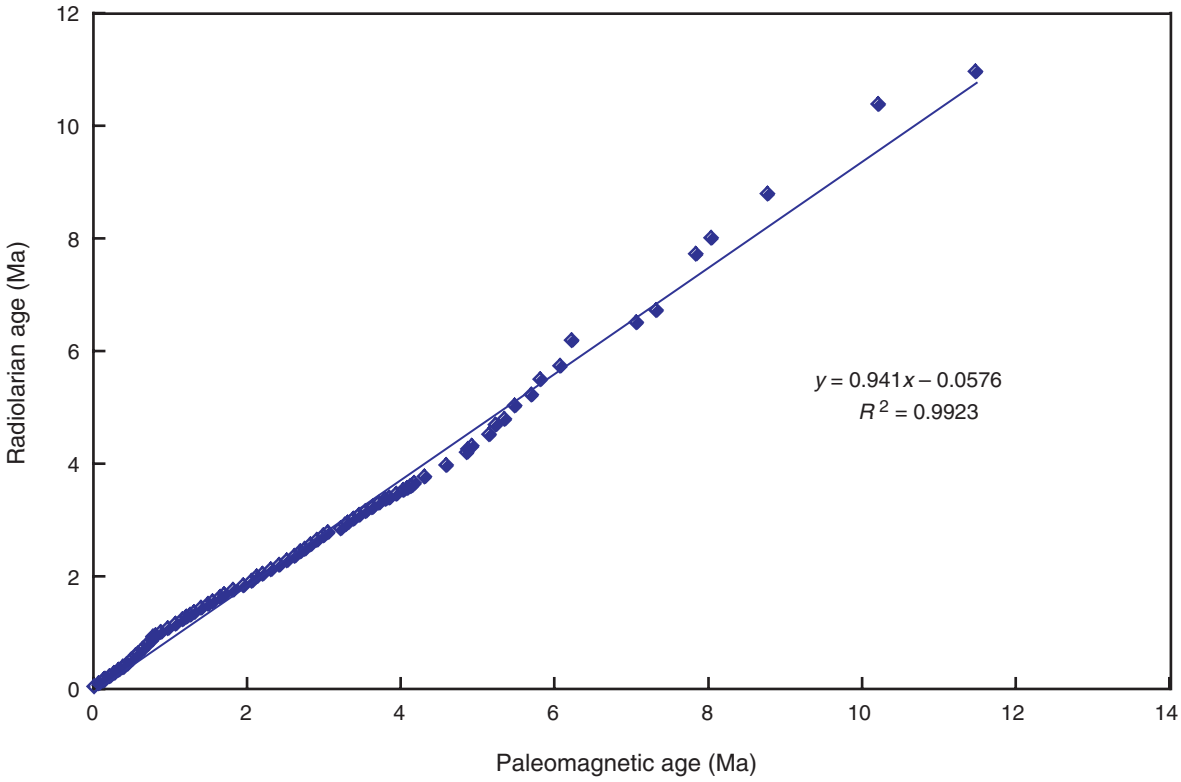

Figure F3. Published and Leg 202, Site 1237 (Shipboard Scientific Party, 2003) radiolarian datums.

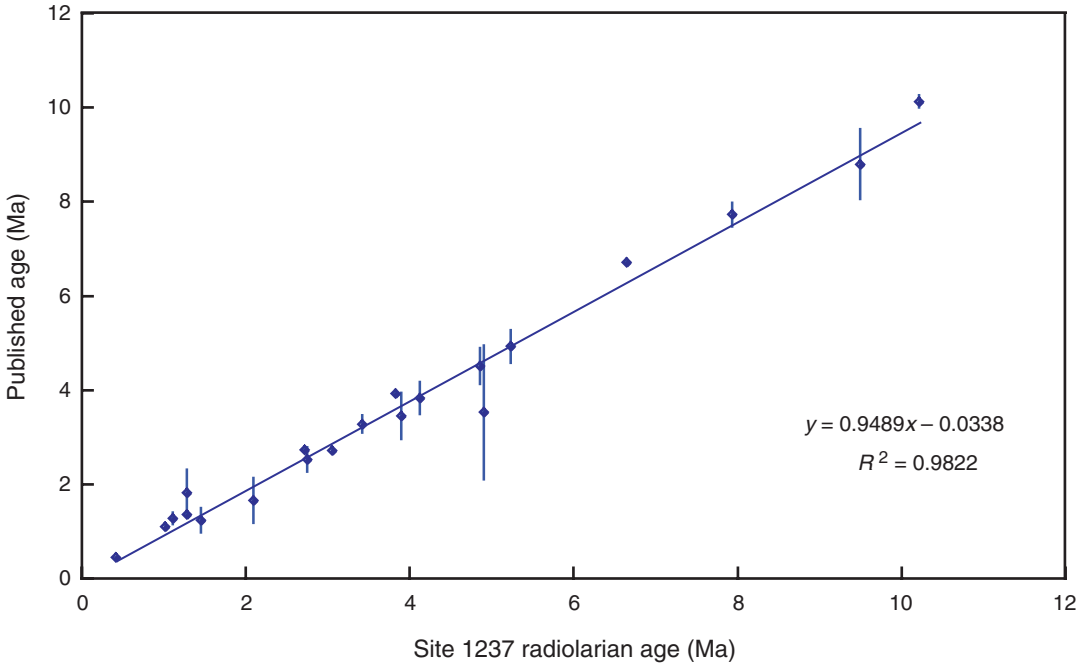

Figure F4. Moore (1995), Sanfilippo and Nigrini (1998), and Shipboard Scientific Party (2003) radiolarian datums.

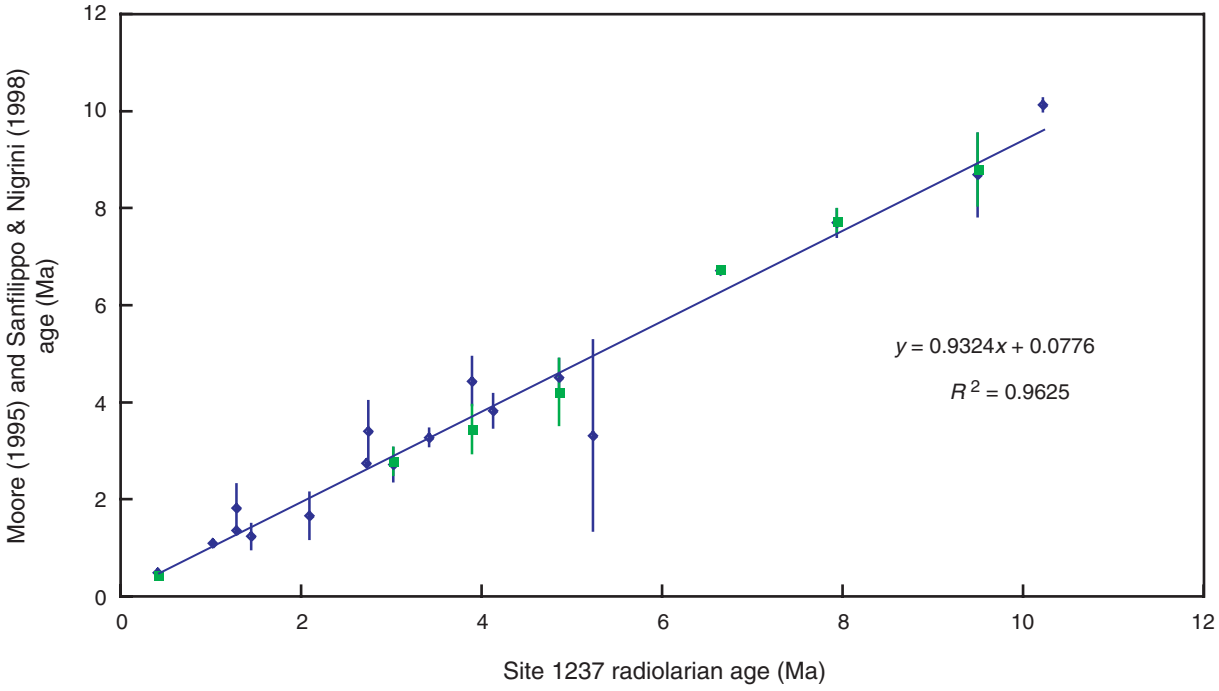

Figure F5. Leg 202, Site 1237 radiolarian biostratigraphy range chart.

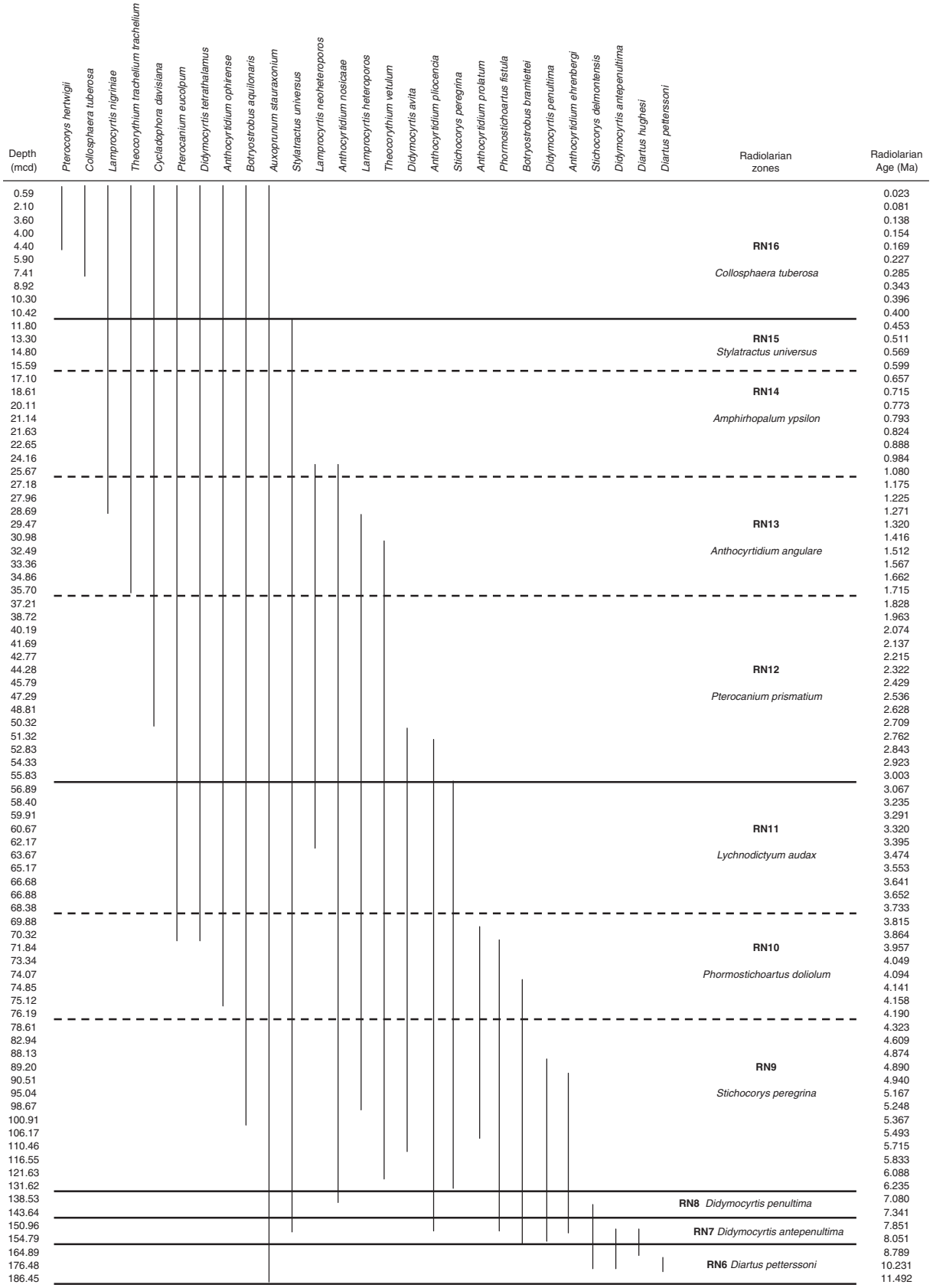

Table T1. Leg 202, Site 1237 radiolarian species range chart. (**See table notes.** Continued on next two pages.)

Zone	Depth (mbsf)	Depth (mcd)	Age (Ma)	Paleomagnetic chronology	Hole, core, section, interval (cm)	Assemblage: Abundance	Assemblage: Preservation	Assemblage: Diversity	*Pterocorys hertwigii*	*Collosphaera tuberosa*	*Lamprocyrtis nigriniae*	*Theocorythium trachelium trachelium*	*Cycladophora davisiana*	*Pterocanium eucolpum*	*Didymocyrtis tetrathalamus*	*Anthocyrtidium ophirense*	*Botryostrobus aquilonaris*	*Axoprunum stauraxonium*	*Stylatractus universus*	*Lamprocyrtis neoheteroporos*	*Anthocyrtidium nosicaae*	*Lamprocyrtis heteroporos*	*Theocorythium vetulum*	*Didymocyrtis avita*	*Anthocyrtidium pliocencia*	*Stichocorys peregrina*	*Anthocyrtidium prolatum*	*Phormostichoartus fistula*	*Botryostrobus bramlettei*	*Didymocyrtis penultima*	*Anthocyrtidium ehrenbergi*	*Stichocorys delmontensis*	*Didymocyrtis antepenultima*	*Diartus hughesi*	*Diartus petterssoni*
RN16 *Collosphaera tuberosa*	0.59	0.59	0.023	Brunhes C1n	1237B-1H-1, 59–61	4	4	4	R	—	C	R	A	R	X	X	A	X																
	2.10	2.10	0.081		1237B-1H-2 59–61	4	4	4	—	—	C	—	A	R	—	X	C	X																		
	3.60	3.60	0.138		1237B-1H-3, 59–61	4	4	4	—	—	C	—	C	R	X	X	C	R																		
	4.00	4.00	0.154		1237D-1H-1, 82–84	4	4	4	—	—	X	R	C/A	R	X	—	X	X																		
	4.90	4.40	0.169		1237D-1H-2, 58–60	5	4	4	R	—	A	R	C	R	X	C	X	X																		
	6.40	5.90	0.227		1237D-1H-3, 58–60	5	4	4	—	—	C	R	C	R	X	—	C	X																		
	7.91	7.41	0.285		1237D-1H-4, 59–61	5	4	4	—	R	X	R	X	R	X	X	X	X																		
	9.42	8.92	0.343		1237D-1H-5, 59–61	4	4	4	—	—	X	R	X	R	X	X	X	X	—																	
	11.40	10.30	0.396		1237C-2H-2, 59–61	4	4	4	—	—	X	R	X	R	X	—	X	X	—																	
	10.92	10.42	0.400		1237D-1H-6, 59–61	4	4	4	—	—	X	R	C/A	R	X	—	X	X	—																	
RN15 *Stylatractus universus*	12.90	11.80	0.453		1237C-2H-3, 59–61	4	4	4	—	—	X	—	C	R	X	X	C	X	X																	
	14.40	13.30	0.511		1237C-2H-4, 59–61	4	4	4	—	—	X	—	C	R	X	—	C	X	X																	
	15.90	14.80	0.569		1237C-2H-5, 59–61	4	4	3	—	—	X	R	X	R	X	X	X	X	X																	
	14.39	15.59	0.599		1237D-2H-2, 59–61	4	4	3	—	—	X	—	X	R	X	X	C	X	X																	
	15.90	17.10	0.657		1237D-2H-3, 59–61	4	3	3	—	—	X	—	X	R	X	—	X	X	X																	
	17.41	18.61	0.715		1237D-2H-4, 59–61	4	4	4	—		X	—	X	—	X	X	X	X	X																	
RN14 *Amphirhopalum ypsilon*	18.91	20.11	0.773	Matuyama	1237D-2H-5, 59–61	4	4	4	—		X	—	C	—	X	X	C	X	X																	
	19.39	21.14	0.793		1237C-3H-1, 59–61	1	1	1	—		—	—	X	—	—	—	—	—	—	—																
	20.43	21.63	0.824		1237D-2H-6, 59–61	4	4	4	—		X	—	X	R	X	X	X	X	X	X	—															
	20.90	22.65	0.888		1237C-3H-2, 59–61	3	3	3	—		C	—	C	R	X	X	A	X	X	X	—															
	22.41	24.16	0.984	C1r.1n	1237C-3H-3, 59–61	3	3	2	—		X		X	R	X	—	A	R	C	—																
	23.92	25.67	1.080		1237C-3H-4, 59–61	4	4	4	—		C	R	C	R	X	X	A	X	C	R	X															
	25.43	27.18	1.175		1237C-3H-5, 59–61	4	3	3			X	—	C/A	R	X	X	A	X	C	R	—															
	25.41	27.96	1.225		1237D-3H-3, 59–61	2	3	2			R	—	X	—	—	—	X	X	A	R	—															
	26.94	28.69	1.271		1237C-3H-6, 59–61	3	3	3			R	—	X	—	—	X	C	X	C	X	—															
RN13 *Anthocyrtidium angulare*	26.92	29.47	1.320	Matuyama	1237D-3H-4, 59–61	3	4	2			—	—		R	X	—	X	X	X	—	—	R	—											
	28.43	30.98	1.416		1237D-3H-5, 59–61	2	3	2			—	—	X	—	X	—	X	X	X	—	—	R	—												
	29.94	32.49	1.512		1237D-3H-6, 59–61	2	3	2			—	—	R	—	X	X	X	X	C	X	—	R	R												
	31.91	33.36	1.567		1237C-4H-3, 59–61	2	2	2			—	—		—	X	—	X	X	X	—	—	—	—												
	33.41	34.86	1.662		1237C-4H-4, 59–61	3	3	3			—	—	X	—	X	—	C	C	A	C	—	R	X												
	33.28	35.70	1.715		1237D-4H-2, 59–61	3	3	3			—	R	C	R	X	X	C	X	X	X	—	R	—												

Table T1 (continued).

Zone	Depth (mbsf)	Depth (mcd)	Age (Ma)	Paleomagnetic chronology	Hole, core, section, interval (cm)	Assemblage: Abundance	Assemblage: Preservation	Assemblage: Diversity	*Pterocorys hertwigii*	*Collosphaera tuberosa*	*Lamprocyrtis nigriniae*	*Theocorythium trachelium trachelium*	*Cycladophora davisiana*	*Pterocanium eucolpum*	*Didymocyrtis tetrathalamus*	*Anthocyrtidium ophirense*	*Botryostrobus aquilonaris*	*Axoprunum stauraxonium*	*Stylatractus universus*	*Lamprocyrtis neoheteroporos*	*Anthocyrtidium nosicaae*	*Lamprocyrtis heteroporos*	*Theocorythium vetulum*	*Didymocyrtis avita*	*Anthocyrtidium pliocencia*	*Stichocorys peregrina*	*Anthocyrtidium prolatum*	*Phormostichoartus fistula*	*Botryostrobus bramlettei*	*Didymocyrtis penultima*	*Anthocyrtidium ehrenbergi*	*Stichocorys delmontensis*	*Didymocyrtis antepenultima*	*Diartus hughesi*	*Diartus petterssoni*
RN12 *Pterocanium prismatium*	34.79	37.21	1.828		1237D-4H-3, 59–61	3	3	2			—	—	X	—	X	—	C	X	X	C	—	R	R												
	36.30	38.72	1.963	C2n	1237D-4H-4, 59–61	3	3	3			—	—	X	—	X	—	C	X	C/A	X	—	X	X												
	37.77	40.19	2.074		1237D-4H-5, 59–61	3	3	3			—	—	X	—	X	—	C/A	X	A	X	X	X	X												
	39.27	41.69	2.137		1237D-4H-6, 59–61	4	3	3			—	—	C/A	R	X	—	A	X	C	X	X	C	X												
	39.90	42.77	2.215		1237C-5H-2, 59–61	4	4	3			—	—	X	—	X	X	C	X	X	C		X	X												
	41.41	44.28	2.322	(C2r.1n)	1237C-5H-3, 59–61	4	3	4			—	—	C	—	X	X	A	X	A	X	X	C	X												
	42.92	45.79	2.429		1237C-5H-4, 59–61	2	3	3			—		X	—	X	X	X	X	C	X		X	X												
	44.42	47.29	2.536		1237C-5H-5, 59–61	4	4	3			—		X	—	—	X	C/A	X	A	X		C	X	—											
	45.94	48.81	2.628		1237C-5H-6, 59–61	3	3	3			—		R	—	X	X	C	X	C	R		X	X	—	—										
	47.45	50.32	2.709	Matuyama	1237C-5H-7, 59–61	3	4	3					R	—	X	X	C/A	X	A	R	X	X	X	—	—										
	45.60	51.32	2.762		1237B-6H-2, 59–61	3	4	3					—	R	R	X	X	X	C	R	X	C	X	X	—										
	47.11	52.83	2.843		1237B-6H-3, 59–61	4	4	3					—	—	R	X	X	X	A	R	X	C	X	X	F	—									
	48.61	54.33	2.923		1237B-6H-4, 59–61	3	3	2					—	—	R	—	X	X	A	R	X	R	X	X		—									
	50.11	55.83	3.003		1237B-6H-5, 59–61	3	3	2						—	R	—	X	X	C/A	X	X	X	X	X	F	—									
	52.42	56.89	3.067	C2An.1n Gauss	1237C-6H-4, 59–61	3	4	3						R	R	X	X	X	C/A	X	X	C	R	X	F	C									
	53.93	58.40	3.235		1237C-6H-5, 59–61	3	3	3						—	R	—	A	X	A	X	X	X	X	X		X									
	55.44	59.91	3.291		1237C-6H-6, 59–61	4	4	4						R	R	—	X	X	A	X	X	C	X	R		X									
	55.10	60.67	3.320		1237B-7H-2, 59–61	3	4	3						R	R	X	X	X	A	R	X	X	R	R		—									
RN11 *Lychnodictyum audax*	56.60	62.17	3.395		1237B-7H-3, 59–61	3	2	3						—	R	X	C	X	C	R	X	X	R	R		R									
	58.10	63.67	3.474		1237B-7H-4, 59–61	1	1	1						—	R	—	—	C	R	—	—	—	—	—		—									
	59.60	65.17	3.553	(C2An.2n)	1237B-7H-5, 59–61	3	3	3						R	—	X	X	X	X	—	—	—	R	—	F	X									
	61.11	66.68	3.641		1237B-7H-6, 59–61	1	1	1						R	—	—	—	X	X	—	—	—	—	—		—									
	61.91	66.88	3.652		1237C-7H-4, 59–61	3	3	3						—	—	—	—	X	X	—	—	—	X	—		—	—								
	63.41	68.38	3.733		1237C-7H-5, 59–61	4	4	4						—	R	X	X	X	C		X	X	R	X		R	—	—							
	64.91	69.88	3.815		1237C-7H-6, 59–61	3	3	3						—	X	—	X	X	C/A		X	—	—	—		—	—	—							
	64.60	70.32	3.864		1237B-8H-2, 59–61	3	3	3						R	X	—	X	X	X		X	—	X	R	R	R	X	R	—						
	66.12	71.84	3.957	C2An.3n Gauss	1237B-8H-3, 59–61	3	3	3						—	—	R	X	R	C		R	—	—	R	R	R	—	R	—						
RN10 *Phormostichoartus doliolum*	67.62	73.34	4.049		1237B-8H-4, 59–61	4	4	4						—	—	X	X	X	C		X	X	R	X	X	R	R	R	—						
	68.38	74.07	4.094		1237C-8H-2, 59–61	3	3	3						—	—	R	R	R	A		R	—	R	R	R	R	R	—	—						
	69.13	74.85	4.141		1237B-8H-5, 59–61	3	3	3						—		X	X	X	C		—	—	R	R	X	C	—	—	X						
	69.45	75.12	4.158		1237C-8H-3, 12–14	3	3	3								X	—	—	C		F	—	R	R	X	C	R	—	—						
	70.52	76.19	4.190		1237D-5H-1, 72–74	3	3	3								—	—	X	C		F	—	—	X	X	A	—	R	—	—					
	72.94	78.61	4.323	Gilbert	1237D-5H-3, 12–14	3	3	3								—	—	X	X		—	—	X	R	C	A	R	—	—	—				
RN9 *Stichocorys peregrina*	76.77	82.94	4.609		1237C-9H-1, 92–94	3	3	3								—	X	—	X		F	—	X	X	C	A	—	—	—	—	—			
	81.96	88.13	4.874		1237C-9H-5, 12–14	3	3	3									X	X	C		—	—	X	X	C	A	R	R	—	—	—			
	82.13	89.20	4.890	C3n.1n	1237D-6H-2, 32–34	4	4	3									X	C	A		F	—	X	X	X	A	—	R	X	C	—			
	83.44	90.51	4.940		1237D-6H-3, 12–14	3	3	3									X	X	X		—	—	X	—	X	A	R	—	—	—	R			

Table T1 (continued).

Zone	Depth (mbsf)	Depth (mcd)	Age (Ma)	Paleomagnetic chronology	Hole, core, section, interval (cm)	Assemblage: Abundance	Assemblage: Preservation	Assemblage: Diversity	*Pterocorys hertwigii*	*Collosphaera tuberosa*	*Lamprocyrtis nigriniae*	*Theocorythium trachelium trachelium*	*Cycladophora davisiana*	*Pterocanium eucolpum*	*Didymocyrtis tetrathalamus*	*Anthocyrtidium ophirense*	*Botryostrobus aquilonaris*	*Axoprunum stauraxonium*	*Stylatractus universus*	*Lamprocyrtis neoheteroporos*	*Anthocyrtidium nosicaae*	*Lamprocyrtis heteroporos*	*Theocorythium vetulum*	*Didymocyrtis avita*	*Anthocyrtidium pliocencia*	*Stichocorys peregrina*	*Anthocyrtidium prolatum*	*Phormostichoartus fistula*	*Botryostrobus bramlettei*	*Didymocyrtis penultima*	*Anthocyrtidium ehrenbergi*	*Stichocorys delmontensis*	*Didymocyrtis antepenultima*	*Diartus hughesi*	*Diartus petterssoni*
RN9 *Stichocorys peregrina*	87.97	95.04	5.167	C3n.2n	1237D-6H-6, 12–14	4	4	4									X	X	C		—	—	X	X	X	C/A	—	—	—	—	R				
	91.45	98.67	5.248		1237C-10H-5, 12–14	3	3	3									—	X	X		X	X	X	—	X	X	R	R	—	—	—				
	92.89	100.91	5.367	C3n.3n	1237D-7H-3, 7–9	4	4	4									X	X	C		X	—	R	X	X	C	R	R	—	—	—				
	98.00	106.17	5.493	C3n.4n	1237C-11H-3, 17–19	3	3	3									—	X	C/A		—	—	X	X	X	C/A	R	R	X	R	R				
	102.39	110.46	5.715	Gilbert	1237D-8H-3, 7–9	3	3	3									—	X	X		X	—	X	R	X	C	—	R	X	—	—				
	107.93	116.55	5.833		1237C-12H-3, 61–63	4	3	3									—	C	C		—	—	—	—	—	X	—	—	X	—	—				
	110.58	121.63	6.088	(C3An.1n)	1237B-13H-1, 58–60	4	3	3										X	X		X	—	R	—	X	R	—	X	X	—	X	—			
	122.42	131.62	6.235	C3An.2n	1237C-13H-5, 58–60	3	3	3										X	X		—	—	—	—	—	R		—	—	—	—	—			
RN8 *Didymocyrtis penultima*	127.48	138.53	7.080		1237C-14H-2, 67–69	3	3	3										X	C		X	—	—		—	—		—	X	—	—	—	—		
	131.09	143.64	7.341	(C3Bn)	1237B-15H-2, 58–60	3	3	3										X	X			—	—		—	—		—	—	X	—	X	—	—	
RN7 *Didymocyrtis antepenultima*	139.91	150.96	7.851	Gilbert C5An.1n to C5r.2n	1237C-15H-4, 58–60	3	3	3										X	C			—			R	—		R	X	X	R	C	—	—	
	142.09	154.79	8.051		1237B-16H-3, 58–60	3	3	3										X	—			—						—	X	X	—	X	X	X	—
RN6 *Diartus petterssoni*	150.09	164.89	8.789		1237B-17H-2, 58–60	2	3	2										X	—									—	—	—	—	X	X	X	—
	160.75	176.48	10.231		1237B-18H-3, 58–60	2	2	2										X	—									—	—	—	—	X	X	—	X
	169.10	186.45	11.492		1237B-19H-2, 5860	1	1	1										X	—									—	—	—	—	—	—	—	—

Notes: Paleomagnetic chronology is based on magnetic stratigraphy from Cande and Kent (1995). Overall preservation, abundance and diversity was designated using numerals between 1 and 5 where 1 = very poor, 2 = poor, 3 = fair, 4 = good, and 5 = very good. R = rare (<10 specimens), X = present (10–100 specimens), C = common (100–200 specimens), A = abundant, (>200 specimens), and — = looked for but not found. Species interval zones were included with the zonal code numbers for clarity. Dashed lines = estimated zone boundaries, solid lines = zones represented by the radiolaria species of Sanfilippo and Nigrini (1998).

Table T2. Leg 202, Site 1237 preliminary ash layer data and Site 1237 observed ash in radiolarian slides. (See table notes. Continued on next two pages.)

Ash layer number	Core, section, interval (cm)	Depth (mcd) Top	Depth (mcd) Bottom	Thickness (cm)	Ash in radiolarian slides A	Ash in radiolarian slides VA
1	**202-1237A- 1H-3, 119–125**	**6.110**	**6.170**	**6**		
1	**202-1237D- 1H-3, 84–90**	**6.150**	**6.210**	**6**		
1	**202-1237C- 1H-5, 14–20**	**6.220**	**6.280**	**6**		
2	202-1237A- Not found	8.200	8.230	3		
2	202-1237C- 1H-6, 62–65					
2	202-1237D- Not found					
3	**2H-5, 9–19**	**19.610**	**19.710**	**10**		
Rad slide	**202-1237C- 3H-1, 59–61**	**21.140**	**21.160**			**X**
3	**3H-1, 48–62**	**21.030**	**21.170**	**14**		
3	**202-1237B- 3H-4, 48–57**	**21.110**	**21.200**	**9**		
4	Not found					
4	202-1237C- Not found	26.320	26.340	2		
4	202-1237D- 3H-2, 46–48					
Rad slide	202-1237C- 3H-5, 59–61	27.180	27.200		X	
5	**202-1237D- 3H-3, 50–60**	**27.870**	**27.970**	**10**		
Rad slide	**3H-3, 59–61**	**27.960**	**27.980**			**X**
5	**202-1237B- Core gap**					
5	**202-1237C- 3H-5, 135–143**	**27.940**	**28.020**	**8**		
6	202-1237B- Not found					
6	Not found	28.080	28.110	3		
6	202-1237D- 3H-3, 71–74					
Wash	202-1237B- (Wash) 4H-1, 0–1	28.800	28.810	1		
	202-1237D- Not found					
7	202-1237B- 4H-1, 33–34	29.130	29.140	1		
7	202-1237C- Not found					
7	202-1237D- Not found					
8	**202-1237B- 4H-1, 52–56**	**29.320**	**29.360**	**4**		
8	**202-1237D- 3H-4, 45–51**	**29.330**	**29.390**	**6**		
Rad slide	**3H-4, 59–61**	**29.470**	**29.490**			**X**
8	**202-1237C- 3H-6, 136–140**	**29.460**	**29.500**	**4**		
9	**202-1237B- 4H-1, 82–86**	**29.620**	**29.660**	**4**		
9	**202-1237D- 3H-4, 76–80**	**29.640**	**29.680**	**4**		
9	**202-1237C- 3H-7, 19–24**	**29.800**	**29.850**	**5**		
Wash	4H-1, 3–7	29.780	29.820	4		
10	202-1237B- Not found					
10	202-1237C- Not found					
10	202-1237D- 3H-4, 100–103	29.880	29.910	3		
Wash	202-1237C- 4H-1, 26–31	30.010	30.060	5		
11	**202-1237B- Not found**					
11	**202-1237C- 4H-1, 85–92**	**30.600**	**30.670**	**7**		
11	**202-1237D- 3H-5, 24–25**	**30.630**	**30.640**	**1**		
Rad slide	3H-5, 59–61	30.980	31.000			X
12	**202-1237B- 4H-2, 110–115**	**31.410**	**31.460**	**5**		
12	**202-1237C- 4H-2, 7–15**	**31.330**	**31.410**	**8**		
12	**202-1237D- 3H-5, 100–107**	**31.390**	**31.460**	**7**		
13	**202-1237B- 4H-3, 7–19**	**31.890**	**32.010**	**12**		
13	**202-1237C- 4H-2, 54–74**	**31.800**	**32.000**	**20**		
13	**202-1237D- 3H-5/6, (5)149–(6)9**	**31.880**	**31.990**	**11**		
14	202-1237B- Not found					
14	202-1237C- Not found					
14	202-1237D- 3H-6, 10–12	32.000	32.020	2		
15	**3H-6, 14–19**	**32.040**	**32.090**	**5**		
15	**202-1237C- 4H-2, 81–85**	**32.070**	**32.110**	**4**		
15	**202-1237B- 4H-3, 35–36**	**32.170**	**32.180**	**1**		
16	**4H-4, 79–86**	**34.130**	**34.200**	**7**		
Rad slide	**202-1237C- 4H-4, 59–61**	**34.860**	**34.880**			**X**
16	Not found					
16	202-1237D- Not found					
17	**202-1237B- 5H-1, 89–92**	**38.160**	**38.190**	**3**		
17	**202-1237C- 4H-6, 87–93**	**38.140**	**38.200**	**6**		
17	**202-1237D- 4H-40, 1–8**	**38.140**	**38.210**	**7**		
18	**202-1237B- 5H-2, 85–91**	**39.640**	**39.700**	**6**		

Table T2 (continued).

Ash layer number	Core, section, interval (cm)	Depth (mcd) Top	Depth (mcd) Bottom	Thickness (cm)	Ash in radiolarian slides A	Ash in radiolarian slides VA
18	**202-1237C- Core gap**					
18	**202-1237D- 4H-5, 0–7**	**39.600**	**39.670**	**7**		
19	**202-1237B- 5H-3, 85–102**	**41.150**	**41.320**	**17**		
19	**202-1237C- 5H-1, 44–61**	**41.110**	**41.280**	**17**		
19	**202-1237D- 4H-5/6, (5)149–(6)25**	**41.090**	**41.350**	**26**		
20	202-1237B- 5H-5, 72–74	44.040	44.060	2		
20	202-1237C- Not found					
20	202-1237D- Core gap					
21	202-1237B- 5H-5, 80–82	44.120	44.140	2		
21	202-1237C- Not found					
21	202-1237D- Core gap					
22	**202-1237B- 5H-5, 112–118**	**44.440**	**44.500**	**6**		
22	**202-1237C- 5H-3, 75–80**	**44.440**	**44.490**	**5**		
22	**202-1237D- Core gap**					
23	202-1237B- 5H-5, 122–129	44.540	44.610	7		
23	202-1237C- Not found					
23	202-1237D- Core gap					
24	202-1237B- 5H-6, 17–20	44.990	45.020	3		
24	202-1237C- C-Not found					
24	202-1237D- Core gap					
25	202-1237C- 5H-6, 31–38	48.530	48.600	7		
25	Core gap					
25	202-1237D- Core gap					
Rad slide	202-1237C- 5H-7, 59–61	50.320	50.340		X	
26	202-1237B- 6H-2, 17–18	50.900	50.910	1		
26	202-1237C- Core gap					
26	202-1237D- Core gap					
27	202-1237B- 6H-2, 20–23	50.930	50.960	3		
27	202-1237C- Core gap					
27	202-1237D- Core gap					
Rad slide	202-1237B- 6H-2, 59–61	51.320	51.340		X	
28	**6H-2, 139–140**	**52.120**	**52.130**	**1**		
28	**202-1237C- 6H-1, 10–28**	**51.870**	**52.050**	**18**		
28	**202-1237D- Core gap**					
29	**202-1237B- 6H-3, 12–14**	**52.360**	**52.380**	**2**		
29	**202-1237C- 6H-1, 44–50**	**52.210**	**52.270**	**6**		
29	**202-1237D- Core gap**					
30	**202-1237B- 6H-3, 40–43**	**52.640**	**52.670**	**3**		
30	**202-1237C- 6H-1, 68–77**	**52.450**	**52.540**	**9**		
30	**202-1237D- Core gap**					
Rad slide	202-1237B- 6H-3, 59–61	52.830	52.850		X	
Rad slide	6H-4, 59–61	54.330	54.350			X
Rad slide	202-1237C- 6H-5, 59–61	58.400	58.420			X
Rad slide	202-1237B- 7H-2, 59–61	60.670	60.690		X	
Rad slide	7H-3, 59–61	62.170	62.190		X	
Rad slide	7H-4, 59–61	63.670	63.690		X	
Rad slide	7H-5, 59–61	65.170	65.190		X	
Rad slide	7H-6, 59–61	66.680	66.700			X
Rad slide	**202-1237C- 7H-4, 59–61**	**66.880**	**66.900**			**X**
31	**202-1237B- 7H-6, 85–88**	**66.940**	**66.970**	**3**		
31	202-1237C- Not found					
31	202-1237D- Core gap					
Rad slide	202-1237C- 7H-5, 59–61	68.380	68.400			X
Rad slide	7H-6, 59–61	69.880	69.900			X
Rad slide	202-1237B- 8H-2, 59–61	70.320	70.340		X	
32	**8H-2, 89–92**	**70.620**	**70.650**	**3**		
32	**202-1237C- 7H-6, 130–140**	**70.590**	**70.690**	**10**		
32	**202-1237D- Core gap**					
Rad slide	202-1237B- 8H-3, 59–61	71.84	71.860		X	
Rad slide	8H-4, 59–61	73.34	73.360		X	
33	**8H-4, 63–70**	**73.380**	**73.450**	**7**		
33	**202-1237C- 8H-1, 141–148**	**73.380**	**73.450**	**7**		

Table T2 (continued).

Ash layer number	Core, section, interval (cm)	Depth (mcd) Top	Depth (mcd) Bottom	Thickness (cm)	Ash in radiolarian slides A	Ash in radiolarian slides VA
33	**202-1237D- Core gap**					
Rad slide	202-1237C- 8H-2, 59–61	74.07	74.090		X	
34	**202-1237B- 9H-5, 0–15**	**85.400**	**85.550**	**15**		
34	**202-1237C- 9H-3, 41–57**	**85.400**	**85.560**	**16**		
34	**202-1237D- Core gap**					
35	**202-1237B- 9H-7, 37–43**	**88.790**	**88.850**	**6**		
35	**202-1237C- 9H-5, 64–72**	**88.650**	**88.730**	**8**		
35	**202-1237D- 6H-1, 127–133**	**88.640**	**88.700**	**6**		
36	202-1237B- Core gap					
36	202-1237C- 9H-6, 21–24	89.730	89.760	3		
36	202-1237D- Not found					
Rad slide	6H-6, 12–14	95.04	95.060		X	
Rad slide	202-1237C- **10H-5, 12–14**	**98.67**	**98.690**			**X**
37	**202-1237B- 10H-6/7, (6)129-(7)9**	**99.580**	**99.890**	**31**		
37	**202-1237C- 10H-5, 93–127**	**99.480**	**99.820**	**34**		
37	**202-1237D- 7H-2, 10–46**	**99.430**	**99.790**	**36**		
38	**202-1237B- 11H-5, 33–41**	**107.040**	**7.120**	**8**		
38	**202-1237C- 11H-3, 91–99**	**106.910**	**106.990**	**8**		
38	**202-1237D- 7H-CC, 17–21**	**106.640**	**106.680**	**4**		
39	**202-1237B- 12H-4, 34–41**	**116.130**	**16.200**	**7**		
39	**202-1237C- 12H-3, 21–26**	**116.150**	**116.200**	**5**		
39	**202-1237D- 8H-6, 120–127**	**116.110**	**116.180**	**7**		
40	**202-1237B- 12H-6, 83–88**	**119.640**	**19.690**	**5**		
40	**202-1237C- 12H-5, 89–93**	**119.830**	**119.870**	**4**		
40	**202-1237D- Core gap**					
41	202-1237B- 13H-2, 123–126	123.800	23.830	3		
41	202-1237C- Core gap					
41	202-1237D- Core gap					
42	202-1237B- 13H-3, 88–95	124.970	25.040	7		
42	202-1237C- Not found					
42	202-1237D- Core gap					
43	**202-1237B- 14H-1, 29–33**	**131.540**	**131.580**	**4**		
43	**202-1237C- 13H-5, 47–49**	**131.510**	**131.530**	**2**		
43	**202-1237D- Core gap**					
Rad slide	202-1237C- 13H-5, 58–60	131.62	131.640		X	
44	**202-1237B- 14H-1, 55–62**	**131.800**	**131.870**	**7**		
44	**202-1237C- 13H-5, 67–75**	**131.710**	**131.790**	**8**		
44	**202-1237D- Core gap**					
45	202-1237B- 14H-1, 109–110	132.340	132.350	1		
45	202-1237C- Not found					
45	202-1237D- Core gap					
46	**202-1237B- 14H-1, 113–114**	**132.380**	**132.390**	**1**		
46	**202-1237C- 13H-5, 123–124**	**132.270**	**132.280**	**1**		
46	**202-1237D- Core gap**					
47	**202-1237B- 14H-2, 76–82**	**133.520**	**133.580**	**6**		
47	**202-1237C- 13H-6, 98–108**	**133.530**	**133.630**	**10**		
47	**202-1237D- Core gap**					
48	**202-1237B- 14H-2, 82–83**	**133.580**	**133.590**	**1**		
48	**202-1237C- 13H-6, 108–109**	**133.630**	**133.640**	**1**		
48	**202-1237D- Core gap**					
49	**202-1237B- 14H-5, 118–123**	**138.450**	**138.500**	**5**		
49	**202-1237C- 14H-2, 52–59**	**138.370**	**138.440**	**7**		
Rad slide	202-1237C- 14H-2, 67–69	138.53	138.550			X
49	**202-1237D- Core gap**					

Notes: Bold = ash layers that could be correlated between holes. A = abundant ash, VA = very abundant ash. Rad slide = radiolarian slide, this study.

Table T3. Median species ages used in this study.

Biostratigraphic event	Paleomagnetism, Leg 202, Site 1237	Age	Difference	Reference for published age
LO *Stylatractus universus*	0.427	0.420	0.007	Sanfilippo and Nigrini, 1998
		0.460	0.033*	Moore, 1995
LO *Lamprocyrtis neoheteroporos*	1.032	1.070	0.038	Moore, 1995
LO *Anthocyrtidium nosicaae*	1.127	1.250	0.123	Nigrini and Caulet, 1988
FO *Lamprocyrtis nigriniae*	1.296	1.330	0.034	Moore, 1995
LO *Lamprocyrtis heteroporos*	1.296	1.790	0.494	Moore, 1995
LO *Theocorythium vetulum*	1.464	1.900	0.436*	Sanfilippo et al., 1985
		1.210	0.254	Moore, 1995
FO *Theocorythium trachelium trachelium*	1.772	1.630	0.142	Moore, 1995
LO *Stichocorys peregrina*	3.035	2.760	0.275*	Sanfilippo and Nigrini, 1998
		2.690	0.345	Moore, 1995
FO *Cycladophora davisiana*	2.735	2.710	0.025	Moore, 1995
LO *Anthocyrtidium pliocencia*	2.802	2.500	0.302	Nigrini and Caulet, 1988
		3.380	0.578*	Moore, 1995
FO *Lamprocyrtis neoheteroporos*	3.434	3.250	0.184	Moore, 1995
LO *Anthocyrtidium prolatum*	3.84	3.900	0.060	Nigrini and Caulet, 1988†
FO *Phormostichoartus fistula*	3.910	3.420	0.490	Sanfilippo and Nigrini, 1998
		4.410	0.500*	Moore, 1995
FO *Amphirhopalum ypsilon*	4.117	3.800	0.317	Moore, 1995
LO *Didymocyrtis penultima*	4.880	4.190	0.690*	Sanfilippo and Nigrini, 1998
		4.490	0.390	Moore, 1995
LO *Anthocyrtidium ehrenbergi*	4.915	3.500	1.415	Nigrini and Caulet, 1988
FO *Lamprocyrtis heteroporos*	5.308	3.290	2.018*	Moore, 1995
		4.900	0.408	Anderson, 1988
Stichocorys delmontensis > *Stichocorys peregrina*	7.080	6.710	–0.370*	Sanfilippo and Nigrini, 1998
		6.685	–0.395	Moore, 1995
LO *Diartus hughesi*	7.951	7.700	0.251	Sanfilippo and Nigrini, 1998
		7.670	0.281*	Moore, 1995
Diartus petterssoni > *Diartus hughesi*	9.510	8.770	0.740	Sanfilippo and Nigrini, 1998
		8.660	0.850*	Moore, 1995
FO *Cyrtocapsella japonica*	10.231	10.100	0.131	Moore, 1995
Absolute mean $\|\Delta m\| = 0.232$				

Notes: * = not used in calculation of absolute mean difference. † = found only in western Pacific Ocean. FO = first occurrence, LO = last occurrence.